The importance of mass accuracy in selected ion monitoring analysis of branched and isoprenoid tetraethers

Nina Davtian, Edouard Bard, Guillemette Ménot, Yoann Fagault

The importance of mass accuracy in selected ion monitoring analysis of branched and isoprenoid tetraethers

Nina Davtian [a,*], Edouard Bard [a], Guillemette Ménot [b], Yoann Fagault [a]

[a] CEREGE, *Aix-Marseille Univ, CNRS, IRD, INRA, Collège de France, 13545 Aix-en-Provence, France*

[b] *Univ Lyon, ENS de Lyon, Université Lyon 1, CNRS, UMR 5276 LGL-TPE, F-69364, Lyon, France*

*Corresponding author. *E-mail address*: davtian@cerege.fr (N. Davtian)

ABSTRACT

Among the new proxies based on the distribution of glycerol dialkyl glycerol tetraethers (GDGTs), the BIT index (Branched and Isoprenoid Tetraether index) is one of the most difficult to determine accurately, as shown by two round-robin GDGT studies. Sensitivity to mass spectrometer settings and tuning, and a diversity of mass spectrometry techniques may explain the relatively large observed interlaboratory scatter. However, the mass defect difference between crenarchaeol and branched GDGTs (brGDGTs) has never been specifically scrutinized. In this study, we analyzed five sediment samples with contrasting BIT values using about 60 *m*/*z* values to assess the shape of GDGT peaks using selected ion monitoring. We then assessed the biases on relative GDGT signals and mass spectrometry-derived BIT values under two scenarios which ignore the systematic mass defect difference between crenarchaeol and brGDGTs. Our results show that approximate mass selection for GDGT analysis using selected ion monitoring generates losses of relative GDGT signals of up to 36%. The observed effects on BIT values are maximal for intermediate BIT values, with shifts of BIT values of ±0.1 unit. The shifts of BIT values due to approximate mass selection are thus not negligible compared to the interlaboratory scatter evidenced by the latest round-robin GDGT study.

Keywords: Mass defect difference, selected ion monitoring, HPLC–APCI-MS, GDGTs, BIT index.

1. Introduction

The development of normal phase high performance liquid chromatography coupled to positive ion atmospheric pressure chemical ionization mass spectrometry (HPLC–APCI-MS) has greatly facilitated the analysis of polar lipids with high molecular weights (Hopmans et al., 2000). Following this analytical development, a number of new proxies based on the relative distributions of glycerol dialkyl glycerol tetraethers (GDGTs) have been developed (Schouten et al., 2013b and References therein). Among the new GDGT-based proxies, the BIT index (Branched and Isoprenoid Tetraether index; Hopmans et al., 2004) has been proposed as a tracer for terrestrial organic carbon in sediments. The BIT index is a ratio that compares the abundance of crenarchaeol, an isoprenoid GDGT produced by *Thaumarchaeota* (e.g., Sinninghe Damsté et al., 2002), with those of branched GDGTs (brGDGTs), which are produced by (acido)bacteria (Weijers et al., 2009; Sinninghe Damsté et al., 2011, 2014). It is noteworthy that the BIT index, while widely determined, needs to be carefully interpreted in order to reconstruct terrigenous fluxes (Schouten et al., 2013b and References therein).

The two international intercomparisons of GDGT measurements (round-robin) have shown specific difficulties associated with calculation of the BIT index (Schouten et al., 2009, 2013a). Escala et al. (2009) have shown that the BIT index, which considers two different families of GDGTs, is particularly sensitive to APCI conditions. Such sensitivity may explain part

of the relatively large interlaboratory scatter of the BIT index, especially for samples with intermediate BIT values (Schouten et al., 2009, 2013a). However, the approximate mass selection for GDGT analysis using selected ion monitoring (SIM) has not yet been explored as a reason for the poor reproducibility between labs of the BIT index. It is noteworthy that while many types of MS and GDGT analysis techniques exist, most laboratories analyzed GDGTs using SIM with single quadrupole mass spectrometers (QMS) during both round-robin GDGT studies (Schouten et al., 2009, 2013a).

Following a review of about three hundred manuscripts where GDGTs were analyzed using SIM with QMS, we have found only a dozen manuscripts (ca. 4%) where *m*/*z* values are written with at least one decimal place (e.g., Herfort et al., 2006; Yang et al., 2011; Basse et al., 2014). In the other manuscripts, the *m*/*z* values are either systematically written as integer numbers (e.g., Cao et al., 2017; Freymond et al., 2017; Naafs et al., 2017), or not indicated at all (e.g., Keisling et al., 2017; Ruan et al., 2017; Woelders et al., 2017). This means that only a few manuscripts clearly reported exact *m*/*z* values rounded up to at least one decimal rather than approximate, integer *m*/*z* values for GDGT analysis using SIM.

In the present study, we analyzed five sediment samples with contrasting BIT values. We selected about 60 *m*/*z* values for GDGT detection using SIM to obtain the relative GDGT signals depending on mass selection. We then assessed the biases on relative GDGT signals and on BIT values

under two scenarios that ignore the systematic mass defect difference between crenarchaeol and brGDGTs.

2. Materials and methods

The mass defect is defined as the exact molecular mass minus the nominal molecular mass – i.e., Mass defect = $M_{exact} - M_{nominal}$. GDGTs are long hydrogenated molecules and their mass defect values are around 1 or more. It should be noted that the mass defect is independent of the protonation – which adds about 1 Da to nominal and exact molecular masses. In this study, the assumption of a unique mass defect for all compounds is referred to as a "unique mass defect scenario".

Taking into account the newest brGDGT isomers (De Jonge et al., 2013; Ding et al., 2016), the BIT index equation of Hopmans et al. (2004) has been redefined as follows:

$$\mathrm{BIT} = \frac{\mathrm{Ia} + \mathrm{IIa_5} + \mathrm{IIIa_5} + \mathrm{IIa_6} + \mathrm{IIIa_6} + \mathrm{IIa_7} + \mathrm{IIIa_7}}{\mathrm{Cren} + \mathrm{Ia} + \mathrm{IIa_5} + \mathrm{IIIa_5} + \mathrm{IIa_6} + \mathrm{IIIa_6} + \mathrm{IIa_7} + \mathrm{IIIa_7}} \quad (1)$$

Roman numerals refer to brGDGT isomers following the nomenclature of Ding et al. (2016). Equation (1) can be simplified as BIT = A/(A+B), with A and B the brGDGTs and crenarchaeol, respectively. In addition, A and B are distinguished by their different mass defects (Table 1).

Five previously analyzed sediment samples with contrasting BIT values were selected: a modern marine sediment from the Bay of Marseille (Mediterranean Sea, 43.26°N, 5.29°E; about 60 m water depth), a modern lacustrine sediment from Lake Chad (LT17, 13°N, 14°E) and three sediment

105 samples from core MD04-2790. The core was retrieved from the continental
106 shelf of the Black Sea (44.21°N, 30.99°E) during the ASSEMBLAGE 1 cruise
107 of R.V. Marion Dufresne. The BIT values of the core and modern marine
108 sediments were previously determined by Ménot and Bard (2012) and
109 Sanchi et al. (2013), respectively. The lacustrine sediment LT17 and the
110 marine sediment from the Bay of Marseille were selected and analyzed as
111 in-house standard sediments to check the absence of instrumental drift in
112 GDGT-derived indices.

113 New aliquots of the modern sediment samples were extracted at
114 CEREGE with DCM:MeOH (9:1, v:v) using an accelerated solvent extractor
115 ASE 350 (Dionex) at 120 °C and 10^7 Pa. Total lipid extracts were separated
116 following the automated procedure established by Sanchi et al. (2013). The
117 polar fractions of the five selected samples were then dissolved in
118 hexane:isopropanol (98.2:1.8, v:v) prior to GDGT analysis on an Agilent
119 1260 Infinity HPLC coupled to a 6120 single QMS installed at CEREGE.
120 The GDGTs were separated using similar chromatographic columns and
121 solvents to Hopmans et al. (2016), as well as the same elution program, but
122 with a 24 min re-equilibration time.

123 The APCI source conditions were: nebulizer pressure, 40 psi;
124 vaporizer temperature, 325 °C; drying gas (N_2) at 4 L/min and 325 °C;
125 capillary voltage, 5 kV (positive mode); corona, 4 μA; fragmentor, 170 V and
126 280 V for the internal standard C_{46} (Huguet et al., 2006) and natural
127 GDGTs, respectively. About 60 *m*/*z* values (42 of them being reported in

128 Supplementary Table S1) were considered for GDGT detection using SIM
129 with a dwell time of 16 ms to assess the shapes of GDGT peaks (Fig. 1). The
130 samples were analyzed five times each. All the analyses were carried out
131 within a few days after an APCI autotune in positive mode, so the APCI
132 source and QMS are assumed to be properly calibrated. The QMS was
133 calibrated by monitoring the *m*/*z* values of four APCI calibration compounds:
134 121.1, 622.0, 922.0 and 1522.0. Because we considered the correct and
135 incorrect *m*/*z* values at the same time, the cleanliness and stability
136 conditions of the APCI source and quadrupole ion optics were not the
137 limiting factors for our study as confirmed by the coherent and systematic
138 differences described below.

139 The mass spectra at the apex of each GDGT peak were averaged over
140 the five replicates of the five selected samples and then normalized to 100%
141 (Fig. 1; Supplementary Table S1). The 5-, 6- and 7-methyl brGDGT isomers
142 were treated as separate compounds due to the improved GDGT separation.
143 The exact BIT values were calculated using equation (1) based on the GDGT
144 peak areas at the *m*/*z* values of 1292.3, 1050.0, 1036.0 and 1022.0 (after, for
145 instance, Herfort et al., 2006; Supplementary Table S2).

146 Two unique mass defects were tested: (i) a unique mass defect of 1.0,
147 which favors brGDGTs over crenarchaeol, and (ii) a unique mass defect of
148 1.3, which favors crenarchaeol over brGDGTs (Fig. 1). The modified BIT
149 values using the unique mass defects of 1.0 and 1.3 were calculated using
150 equation (1) based on the GDGT peak areas at the *m*/*z* values of 1292.0,

1050.0, 1036.0 and 1022.0, and at the *m*/*z* values of 1292.3, 1050.3, 1036.3 and 1022.3, respectively (Supplementary Table S2). All single-ion chromatograms were obtained using *m*/*z* windows restricted to, for instance, 1050.3–1050.3 to extract the ion at *m*/*z* 1050.3 only. The shifts in BIT values were then determined for each unique mass defect and each sample as the modified BIT values minus the exact BIT values – i.e., ΔBIT = Modified BIT value – Exact BIT value. Errors on GDGT signals and BIT values were calculated based on the five replicates per sample and propagated to the shifts in BIT values using the variance formula. The biases on GDGT signals and BIT values were assessed with paired Student's *t*-tests, which were considered significant if $p < 0.05$.

3. Results and discussion

Under the two unique mass defect scenarios, the relative losses of GDGT signals were calculated using the GDGT peak areas (Table 2). A deviation of 0.2–0.3 Da from the exact molecular mass generated losses of relative GDGT signals between 35 and 36% for crenarchaeol, and between 18 and 27% for brGDGTs (Table 2; all paired Student's *t*-tests on GDGT peak areas with $p < 0.01$). Therefore, for any given sample processing technique, chromatographic method, properly calibrated MS, mass setting and MS technique (e.g., Escala et al., 2009; Schouten et al., 2009, 2013), not taking into account the mass defect difference between crenarchaeol and brGDGTs is indeed sufficient to obtain different GDGT relative responses

and thus different BIT values. It is noteworthy that this caveat applies not only to the BIT index (Fig. 2; Table 3), but also to all GDGT-based indices that consider both isoprenoid GDGTs and brGDGTs.

Shifts in BIT values varied between 0.013 and 0.093 using a unique mass defect of 1.0, and between –0.055 and –0.011 using a unique mass defect of 1.3 (Fig. 2; Table 3; all paired Student's *t*-tests on BIT values with $p < 0.01$). Under both unique mass defect scenarios, the highest shifts in BIT values occurred for the sediment samples from the core MD04-2790, which also had intermediate BIT values (Fig. 2; Table 3). Our results are consistent with those from the two round-robin GDGT studies, which gave higher BIT index scatter for samples with intermediate BIT values than they did for samples with extreme BIT values (Schouten et al., 2009, 2013a). Theoretically, the observed shifts in BIT values are explained by a reduction by 35% of the relative crenarchaeol signal using the unique mass defect of 1.0, and by a general reduction by 21% of the relative brGDGT signal using the unique mass defect of 1.3 (Fig. 2).

To assess the severity of the observed and estimated shifts in BIT values due to approximate mass selection, these shifts are compared with the 95% confidence intervals of interlaboratory means for single QMS only based on the latest round-robin GDGT study (Schouten et al., 2013a). The observed biases on BIT values for the five selected sediment samples were generally larger than the interlaboratory scatter of the relevant round-robin samples for single QMS only (Fig. 2). The observed biases on BIT values are

197 also not negligible compared to the interlaboratory scatter for all MS types
198 (Schouten et al., 2013a). This suggests that approximate mass selection
199 probably contributes to interlaboratory differences.

200 Laboratories 16, 18, 23 and 25 summed $[M+H]^+$ and $[M+H+1]^+$ ions –
201 protonated molecule and first isotope peak with one ^{13}C atom – for BIT
202 index calculations instead of $[M+H]^+$ ions only during the latest round-robin
203 GDGT study (Schouten et al., 2013a), which leads to another bias due to the
204 various numbers of carbon atoms between the different GDGTs. To assess
205 this bias, the abundances of $[M+H+1]^+$ ions relative to $[M+H]^+$ ions were
206 calculated for the GDGTs included in the BIT index (Table 1) and then used
207 to theoretically estimate the shifts in BIT values depending on the initial
208 BIT index value. The calculated shifts reach a maximal value of –0.03 for an
209 initial BIT index value close to 0.5 (Fig. 2), which means that the most likely
210 sources of bias in addition to approximate mass selection are, among others,
211 the diversity of APCI parameters and MS types (e.g., Escala et al., 2009;
212 Schouten et al., 2009, 2013).

213

214 **4. Conclusions and perspectives**

215 The results obtained from five sediment samples showed that not
216 taking into account the systematic mass defect difference between
217 crenarchaeol and brGDGTs generated shifts in BIT values of up to ±0.1 unit.
218 The observed shifts in BIT values represent a non-negligible proportion of
219 the interlaboratory scatter. A round-robin GDGT study focusing on mass

selection for SIM experiments would greatly help to assess the contribution of approximate mass selection to the interlaboratory scatter of BIT values.

Acknowledgements

Work at CEREGE is supported by the Collège de France and BNP-Paribas Foundation (project CPATEMP). N.D. expresses her thanks to the Ecole Normale Supérieure de Lyon for providing PhD salary support. The authors thank the reviewers of an earlier version of this paper.

Appendix A. Supplementary material

Associate Editor–**Ann Pearson**

References

Basse, A., Zhu, C., Versteegh, G.J.M., Fischer, G., Hinrichs, K.-U., Mollenhauer, G., 2014. Distribution of intact and core tetraether lipids in water column profiles of suspended particulate matter off Cape Blanc, NW Africa. Organic Geochemistry 72, 1–13.

Cao, J., Rao, Z., Jia, G., Xu, Q., Chen, F., 2017. A 15 ka pH record from an alpine lake in north China derived from the cyclization ratio index of aquatic brGDGTs and its paleoclimatic significance. Organic Geochemistry 109, 31–46.

De Jonge, C., Hopmans, E.C., Stadnitskaia, A., Rijpstra, W.I.C., Hofland, R., Tegelaar, E., Sinninghe Damsté, J.S., 2013. Identification of novel penta- and hexamethylated branched glycerol dialkyl glycerol tetraethers in peat using HPLC–MS^2, GC–MS and GC–SMB-MS. Organic Geochemistry 54, 78–82.

Ding, S., Schwab, V.F., Ueberschaar, N., Roth, V.-N., Lange, M., Xu, Y., Gleixner, G., Pohnert, G., 2016. Identification of novel 7-methyl and cyclopentanyl branched glycerol dialkyl glycerol tetraethers in lake sediments. Organic Geochemistry 102, 52–58.

Escala, M., Fietz, S., Rueda, G., Rosell-Melé, A., 2009. Analytical considerations for the use of the paleothermometer Tetraether $Index_{86}$ and the branched vs isoprenoid tetraether index regarding the choice of cleanup and instrumental conditions. Analytical Chemistry 81, 2701–2707.

Freymond, C.V., Peterse, F., Fischer, L.V., Filip, F., Giosan, L., Eglinton, T.I., 2017. Branched GDGT signals in fluvial sediments of the Danube River basin: method comparison and longitudinal evolution. Organic Geochemistry 103, 88–96.

Herfort, L., Schouten, S., Boon, J.P., Sinninghe Damsté, J.S., 2006. Application of the TEX_{86} temperature proxy to the southern North Sea. Organic Geochemistry 37, 1715–1726.

Hopmans, E.C., Schouten, S., Pancost, R.D., van der Meer, M.T.J., Sinninghe Damsté, J.S., 2000. Analysis of intact tetraether lipids in

archaeal cell material and sediments by high performance liquid chromatography/atmospheric pressure chemical ionization mass spectrometry. Rapid Communications in Mass Spectrometry 14, 585–589.

Hopmans, E.C., Schouten, S., Sinninghe Damsté, J.S., 2016. The effect of improved chromatography on GDGT-based palaeoproxies. Organic Geochemistry 93, 1–6.

Hopmans, E.C., Weijers, J.W.H., Schefuß, E., Herfort, L., Sinninghe Damsté, J.S., Schouten, S., 2004. A novel proxy for terrestrial organic matter in sediments based on branched and isoprenoid tetraether lipids. Earth and Planetary Science Letters 224, 107–116.

Huguet, C., Hopmans, E.C., Febo-Ayala, W., Thompson, D.H., Sinninghe Damsté, J.S., Schouten, S., 2006. An improved method to determine the absolute abundance of glycerol dibiphytanyl glycerol tetraether lipids. Organic Geochemistry 37, 1036–1041.

Keisling, B.A., Castañeda, I.S., Brigham-Grette, J., 2017. Hydrological and temperature change in Arctic Siberia during the intensification of Northern Hemisphere Glaciation. Earth and Planetary Science Letters 457, 136–148.

Ménot, G., Bard, E., 2012. A precise search for drastic temperature shifts of the past 40,000 years in southeastern Europe. Paleoceanography 27, PA2210.

287 Naafs, B.D.A., Inglis, G.N., Zheng, Y., Amesbury, M.J., Biester, H., Bindler,
288 R., Blewett, J., Burrows, M.A., del Castillo Torres, D., Chambers,
289 F.M., Cohen, A.D., Evershed, R.P., Feakins, S.J., Gałka, M., Gallego-
290 Sala, A., Gandois, L., Gray, D.M., Hatcher, P.G., Honorio Coronado,
291 E.N., Hughes, P.D.M., Huguet, A., Könönen, M., Laggoun-Défarge, F.,
292 Lähteenoja, O., Lamentowicz, M., Marchant, R., McClymont, E.,
293 Pontevedra-Pombal, X., Ponton, C., Pourmand, A., Rizzuti, A.M.,
294 Rochefort, L., Schellekens, J., De Vleeschouwer, F., Pancost, R.D.,
295 2017. Introducing global peat-specific temperature and pH
296 calibrations based on brGDGT bacterial lipids. Geochimica et
297 Cosmochimica Acta 208, 285–301.
298 Ruan, J., Huang, Y., Shi, X., Liu, Y., Xiao, W., Xu, Y., 2017. Holocene
299 variability in sea surface temperature and sea ice extent in the
300 northern Bering Sea: a multiple biomarker study. Organic
301 Geochemistry 113, 1–9.
302 Sanchi, L., Ménot, G., Bard, E., 2013. An automated purification method for
303 archaeal and bacterial tetraethers in soils and sediments. Organic
304 Geochemistry 54, 83–90.
305 Schouten, S., Hopmans, E.C., Rosell-Melé, A., Pearson, A., Adam, P.,
306 Bauersachs, T., Bard, E., Bernasconi, S.M., Bianchi, T.S., Brocks,
307 J.J., Carlson, L.T., Castañeda, I.S., Derenne, S., Selver, A.D., Dutta,
308 K., Eglinton, T., Fosse, C., Galy, V., Grice, K., Hinrichs, K.-U., Huang,
309 Y., Huguet, A., Huguet, C., Hurley, S., Ingalls, A., Jia, G., Keely, B.,

Knappy, C., Kondo, M., Krishnan, S., Lincoln, S., Lipp, J., Mangelsdorf, K., Martínez-García, A., Ménot, G., Mets, A., Mollenhauer, G., Ohkouchi, N., Ossebaar, J., Pagani, M., Pancost, R.D., Pearson, E.J., Peterse, F., Reichart, G.-J., Schaeffer, P., Schmitt, G., Schwark, L., Shah, S.R., Smith, R.W., Smittenberg, R.H., Summons, R.E., Takano, Y., Talbot, H.M., Taylor, K.W.R., Tarozo, R., Uchida, M., van Dongen, B.E., Van Mooy, B.A.S., Wang, J., Warren, C., Weijers, J.W.H., Werne, J.P., Woltering, M., Xie, S., Yamamoto, M., Yang, H., Zhang, C.L., Zhang, Y., Zhao, M., Sinninghe Damsté, J.S., 2013a. An interlaboratory study of TEX_{86} and BIT analysis of sediments, extracts, and standard mixtures. Geochemistry, Geophysics, Geosystems 14, 5263–5285.

Schouten, S., Hopmans, E.C., Sinninghe Damsté, J.S., 2013b. The organic geochemistry of glycerol dialkyl glycerol tetraether lipids: a review. Organic Geochemistry 54, 19–61.

Schouten, S., Hopmans, E.C., van der Meer, J., Mets, A., Bard, E., Bianchi, T.S., Diefendorf, A., Escala, M., Freeman, K.H., Furukawa, Y., Huguet, C., Ingalls, A., Ménot-Combes, G., Nederbragt, A.J., Oba, M., Pearson, A., Pearson, E.J., Rosell-Melé, A., Schaeffer, P., Shah, S.R., Shanahan, T.M., Smith, R.W., Smittenberg, R., Talbot, H.M., Uchida, M., Van Mooy, B.A.S., Yamamoto, M., Zhang, Z., Sinninghe Damsté, J.S., 2009. An interlaboratory study of TEX_{86} and BIT analysis using

high-performance liquid chromatography–mass spectrometry. Geochemistry, Geophysics, Geosystems 10, Q03012.

Sinninghe Damsté, J.S., Rijpstra, W.I.C., Hopmans, E.C., Foesel, B.U., Wüst, P.K., Overmann, J., Tank, M., Bryant, D.A., Dunfield, P.F., Houghton, K., Stott, M.B., 2014. Ether- and ester-bound *iso*-diabolic acid and other lipids in members of *Acidobacteria* subdivision 4. Applied and Environmental Microbiology 80, 5207–5218.

Sinninghe Damsté, J.S., Rijpstra, W.I.C., Hopmans, E.C., Weijers, J.W.H., Foesel, B.U., Overmann, J., Dedysh, S.N., 2011. 13,16-dimethyl octacosanedioic acid (*iso*-diabolic acid), a common membrane-spanning lipid of *Acidobacteria* subdivisions 1 and 3. Applied and Environmental Microbiology 77, 4147–4154.

Sinninghe Damsté, J.S., Schouten, S., Hopmans, E.C., Duin, A.C.T. van, Geenevasen, J.A.J., 2002. Crenarchaeol: the characteristic core glycerol dibiphytanyl glycerol tetraether membrane lipid of cosmopolitan pelagic crenarchaeota. Journal of Lipid Research 43, 1641–1651.

Weijers, J.W.H., Panoto, E., van Bleijswijk, J., Schouten, S., Rijpstra, W.I.C., Balk, M., Stams, A.J.M., Sinninghe Damsté, J.S., 2009. Constraints on the biological source(s) of the orphan branched tetraether membrane lipids. Geomicrobiology Journal 26, 402–414.

Woelders, L., Vellekoop, J., Kroon, D., Smit, J., Casadío, S., Prámparo, M.B., Dinarès-Turell, J., Peterse, F., Sluijs, A., Lenaerts, J.T.M., Speijer,

R.P., 2017. Latest Cretaceous climatic and environmental change in the South Atlantic region. Paleoceanography 32, 466–483.

Yang, H., Ding, W., Zhang, C.L., Wu, X., Ma, X., He, G., Huang, J., Xie, S., 2011. Occurrence of tetraether lipids in stalagmites: implications for sources and GDGT-based proxies. Organic Geochemistry 42, 108–115.

Figure captions

Fig. 1. Examples of averaged mass spectra normalized to 100% of (A) crenarchaeol and of (B) brGDGT-Ia for the sediment sample at 2860 cm depth in core MD04-2790. The error bars correspond to the standard deviations (σ) of the averaged relative GDGT signals per mass (mean value ± 2σ, n = 5). The blue and brown dashed lines describe the scenarios that consider a unique mass defect (ΔM) of 1.0 and 1.3, respectively. The black curves represent the Gaussian functions fitted to the averaged mass spectra so that the shapes of GDGT peaks are more apparent.

Fig. 2. Shifts in BIT values (ΔBIT) vs exact mass spectrometry-based BIT values according to the unique mass defect (1.0 or 1.3). The blue and brown symbols indicate the results from five sediment samples. The horizontal error bars correspond to the standard deviations (σ) of the exact BIT values indicated in Table 3 (mean value ± 2σ, n = 5). The vertical error bars correspond to the standard deviations of the ΔBIT values, which were determined by propagating the standard deviations shown in Table 3 using the variance formula (mean value ± 2σ, n = 5). The blue and brown solid curves indicate the theoretical results for given losses of crenarchaeol and brGDGT signals, respectively. The dark red solid curves indicate the theoretical results when $[M+H]^+$ and $[M+H+1]^+$ ions – protonated molecule and first isotope peak with one ^{13}C atom, respectively – are summed for BIT index calculations instead of $[M+H]^+$ ions only. The colored double arrows

384 indicate the 95% confidence intervals ($\pm t \times SD/\sqrt{n}$, with $t = 2.12$ the t-
385 statistic value for a two-sided 95% confidence interval with 16 degrees of
386 freedom, SD the standard deviation and $n = 17$) of interlaboratory means for
387 single quadrupole mass spectrometers only from the latest round-robin
388 GDGT study (Schouten et al., 2013a). The x-axis positions of the colored
389 double arrows correspond to the averaged interlaboratory BIT values for
390 single quadrupole mass spectrometers only.
391
392 **Table captions**
393 **Table 1**
394 Molecule names, nominal and exact masses of $[M]^+$ and $[M+H]^+$ ions – non-
395 protonated and protonated molecules, respectively – mass defects of $[M+H]^+$
396 ions and abundances of $[M+H+1]^+$ ions – first isotope peak with one ^{13}C
397 atom – relative to $[M+H]^+$ ions. The compounds are indicated following the
398 nomenclature of Ding et al. (2016). All masses and mass defects shown here
399 assume GDGTs with only ^{12}C, ^{1}H and ^{16}O isotopes. Note that the mass
400 defect is independent of the protonation, which adds about 1 Da to both
401 nominal and exact molecular masses.
402
403 **Table 2**
404 Relative losses of GDGT signals (in %) of five sediment samples using the
405 unique mass defects of 1.0 and 1.3 for crenarchaeol and brGDGTs,
406 respectively. The errors correspond to the standard deviations (σ) per

compound and per sample (mean value ± 2σ, n = 5). The compounds are indicated following the nomenclature of Ding et al. (2016).

Table 3

Exact and modified mass spectrometry-based BIT values of five sediment samples according to the unique mass defect (1.0 or 1.3). The errors correspond to the standard deviations (σ) per scenario and per sample (mean value ± 2σ, n = 5).

Figure 1

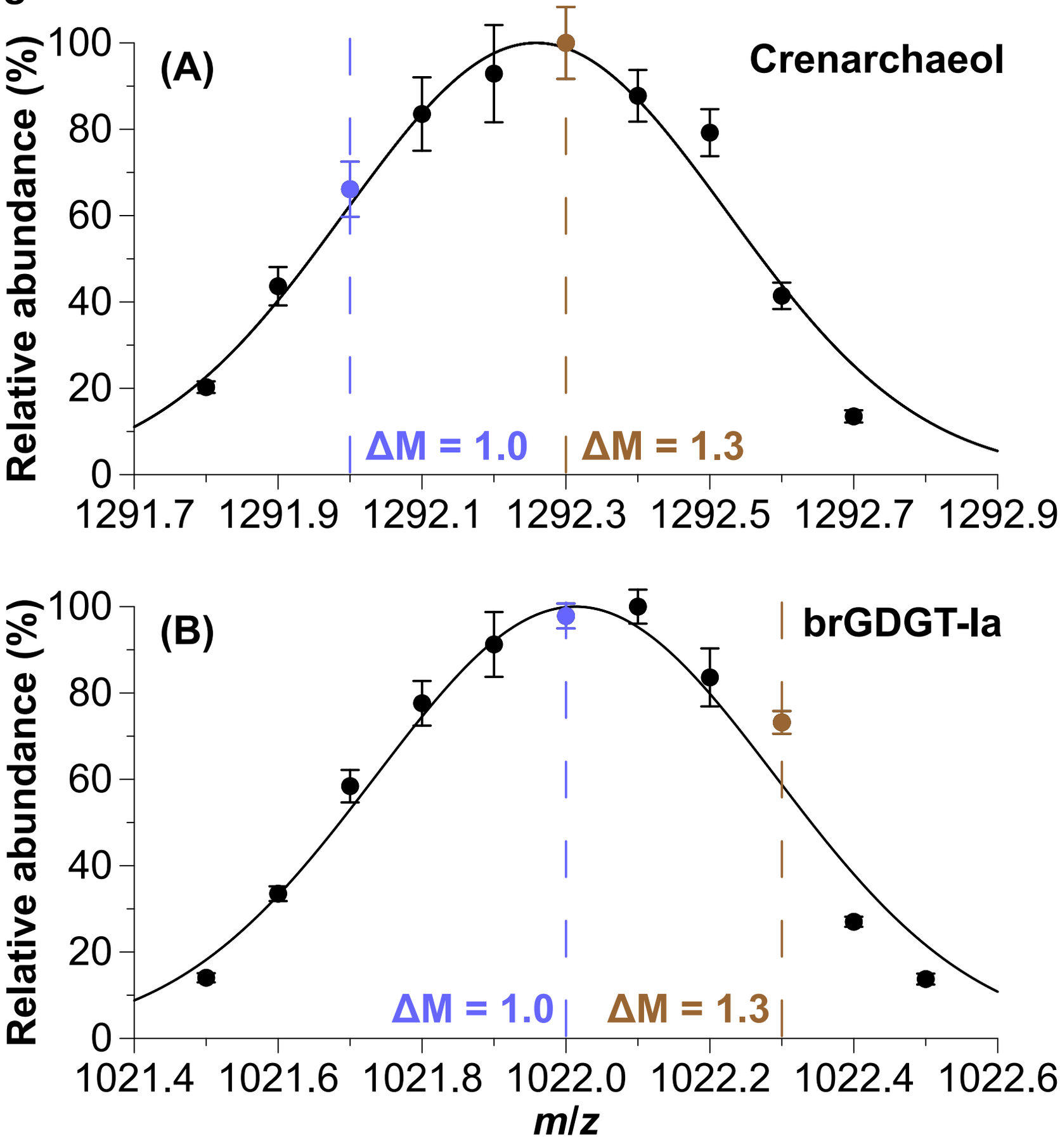
(A)
Crenarchaeol
Relative abundance (%)
100
80
60
40
20
0
ΔM = 1.0
ΔM = 1.3
1291.7
1291.9
1292.1
1292.3
1292.5
1292.7
1292.9
(B)
brGDGT-Ia
Relative abundance (%)
100
80
60
40
20
0
ΔM = 1.0
ΔM = 1.3
1021.4
1021.6
1021.8
1022.0
1022.2
1022.4
1022.6
m/z

Figure 2

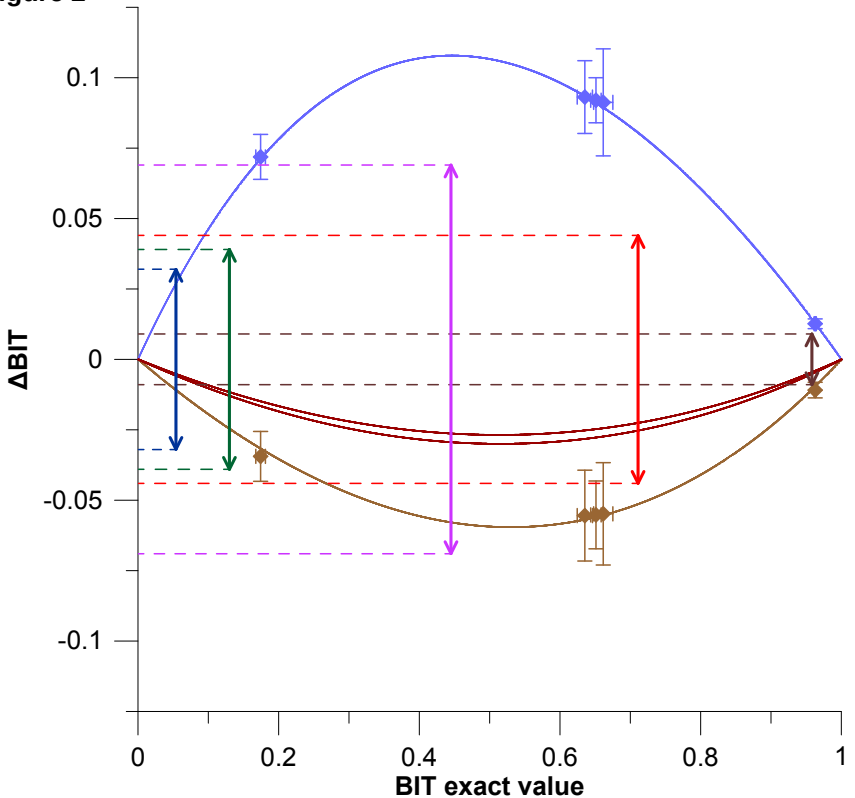

Observations and theoretical estimations

- Unique mass defect = 1.0
- Unique mass defect = 1.3
- -35% crenarchaeol area
- -21% brGDGTs area
- Summing $[M+H]^+$ and $[M+H+1]^+$ ions (cases with only brGDGTs-Ia or -IIIa)

95% confidence limits round-robin study 2011
Single quadrupole mass spectrometers only

- Sediment A
- Sediment B
- Sediment C
- Mixture D
- Mixture E

Table 1 - revised

Molecule name	Nominal mass for $[M]^+$	Nominal mass for $[M+H]^+$	Exact mass for $[M+H]^+$	Mass defect for $[M+H]^+$	$[M+H+1]^+/[M+H]^+$ ions
Crenarchaeol/Crenarchaeol regio-isomer	1290	1291	1292.2444	1.2444	0.946
brGDGT-IIIa_5/brGDGT-IIIa_6/brGDGT-IIIa_7	1048	1049	1050.0488	1.0488	0.748
brGDGT-IIa_5/brGDGT-IIa_6/brGDGT-IIa_7	1034	1035	1036.0325	1.0325	0.737
brGDGT-Ia	1020	1021	1022.0166	1.0166	0.726

Table 2

Sample	Ia	IIa_5	IIa_6	IIa_7	$IIIa_5$	$IIIa_6$	$IIIa_7$	Cren
Bay of Marseille	27 ± 1	24 ± 6	20 ± 5	21 ± 8	20 ± 1	20 ± 4	25 ± 4	35 ± 2
Lake Chad LT17	25 ± 2	21 ± 2	21 ± 4	23 ± 7	20 ± 4	21 ± 2	21 ± 3	35 ± 2
MD04-2790 2851 cm	26 ± 2	21 ± 4	22 ± 2	23 ± 7	19 ± 1	20 ± 2	21 ± 5	36 ± 3
MD04-2790 2860 cm	27 ± 2	22 ± 5	22 ± 4	25 ± 10	19 ± 3	18 ± 4	18 ± 8	35 ± 1
MD04-2790 2870 cm	26 ± 3	22 ± 2	20 ± 2	26 ± 3	19 ± 2	20 ± 4	23 ± 11	35 ± 2

Table 3

Sample	Exact value	Unique mass defect = 1.0	Unique mass defect = 1.3
Bay of Marseille	0.174 ± 0.007	0.246 ± 0.004	0.140 ± 0.006
Lake Chad LT17	0.963 ± 0.002	0.976 ± 0.001	0.952 ± 0.002
MD04-2790 2851 cm	0.661 ± 0.014	0.753 ± 0.013	0.607 ± 0.012
MD04-2790 2860 cm	0.635 ± 0.011	0.728 ± 0.007	0.580 ± 0.012
MD04-2790 2870 cm	0.651 ± 0.007	0.743 ± 0.003	0.596 ± 0.010